

Primary Structure and Properties of Helothermine, a Peptide Toxin that Blocks Ryanodine Receptors

Jeffery Morrisette,* Jörn Krätzschar,† Bernard Haendler,‡ Roque El-Hayek,* Javier Mochca-Morales,§ Brian M. Martin,|| Jitandrakumar R. Patel,* Richard L. Moss,* Wolf-Dieter Schleuning,‡ Roberto Coronado,* and Lourival D. Possani§

*Department of Physiology, University of Wisconsin School of Medicine, Madison, Wisconsin 53706 USA; †Research Laboratories of Schering AG, D-13342 Berlin, Germany; ‡Department of Biochemistry, Institute of Biotechnology, Universidad Nacional Autónoma de México, Cuernavaca 62271, México; and ||NINCDS, DMNB, National Institutes of Health, Bethesda, Maryland 20205 USA

ABSTRACT Helothermine, a protein from the venom of the Mexican beaded lizard (*Heloderma horridum horridum*), was found to inhibit [³H]ryanodine binding to cardiac and skeletal sarcoplasmic reticulum, to block cardiac and skeletal ryanodine receptor channels incorporated into planar bilayers, and to block Ca²⁺-induced Ca²⁺ release triggered by photolysis of nitr-5 in saponin-permeabilized trabeculae from rat ventricle. Cloning of the helothermine cDNA revealed that the protein is composed of 223 amino acids with a molecular mass of 25,376 daltons, and apparently is stabilized by eight disulfide bridges. The peptide sequence showed significant homology with a family of cysteine-rich secretory proteins found in the male genital tract and in salivary glands. The interaction of helothermine and ryanodine receptors should serve to define functional domains within the channel structure involved in the control of Ca²⁺ release from sarcoplasmic reticulum.

INTRODUCTION

The structure of the tetrameric ryanodine receptor and its associated Ca²⁺ channel function are critical in understanding how Ca²⁺ signals are generated inside cells. In muscle, this channel controls the release of Ca²⁺ from intracellular stores when cells are stimulated by voltage and inotropic agents (Coronado et al., 1994). A similar functional role is suspected in many other cell types where ryanodine receptors are expressed (Sorrentino and Volpe, 1993; McPherson and Campbell, 1993; Coronado et al., 1994). Structural features of the tetrameric receptor include four radial canals or pathways that apparently empty into the myoplasm and that connect together to form a single pathway that empties into the sarcoplasmic reticulum (SR) lumen (Wagenknecht et al., 1989). Whether these features represent the true pathways for Ca²⁺ flow and, thus, are part of the pore structure, is unknown. Domains within the peptide sequence of the ryanodine receptor that form binding sites for Ca²⁺ and ryanodine, two ligands that affect the gating state of the protein, also have been identified (Chen et al., 1992; Callaway et al., 1994). So far, the alkaloid ryanodine is the only molecular probe of the channel's structure because it is highly specific and its binding kinetics are sensitive to ligands that open and close the channel (Wang et al., 1993). Purification and molecular characterization of additional ligands affecting specific domains of the ryanodine receptor should provide clues about the pore structure, conformational states, and ligand-binding sites controlling Ca²⁺-induced Ca²⁺ release.

Peptide toxins targeted against ion channels are ideally suited to relate channel structure to ion flow and gating (MacKinnon and Miller, 1989; Giangiacomo et al., 1993). Although a majority of toxins interact with channels of surface membranes (Adams and Swanson, 1994), some scorpion venoms contain peptides specifically targeted against intracellular channels such as the ryanodine receptor (Valdivia et al., 1991, 1992). Here we report that helothermine, a peptide toxin from the salivary secretion of the Mexican beaded lizard *Heloderma horridum horridum* (Mochca-Morales et al., 1990), also appears to target the ryanodine receptor. Molecular cloning established that helothermine is different from other peptide toxins because its primary structure seems to be unrelated to toxins of Na⁺, K⁺, or other channels. In previous studies, a target site for helothermine could not be identified because the toxin did not interact with any of the known cardiac muscle cell ionic currents, including the voltage-dependent Na⁺ and Ca²⁺ currents (Mochca-Morales et al., 1990).

MATERIALS AND METHODS

Purification of helothermine

Helothermine was purified from the salivary secretion of animals kept alive in the laboratory as described previously (Mochca-Morales et al., 1990). Pure toxin was reduced and carboxymethylated (Martin et al., 1988). Peptidic fragments were generated by cyanogen bromide cleavage and by tryptic digestion as described previously (Possani et al., 1985; 1992). Peptides were separated by HPLC, and their amino acid sequences were obtained by automatic Edman degradation using an Applied Biosystems microsequencer (model 470A, Foster City, CA).

Molecular cloning of helothermine

RNA was prepared from the salivary glands of the Mexican beaded lizard *Heloderma horridum horridum* after the guanidinium isothiocyanate procedure according to Sambrook et al. (1989). Poly(A)⁺ RNA was obtained

Received for publication 11 October 1994 and in final form 3 March 1995.

Address reprint requests to Roberto Coronado, Department of Physiology, University of Wisconsin School of Medicine, 1300 University Avenue, Madison, WI 53705. Tel.: 608-263-7487; Fax: 608-262-2327; E-mail: blmlab@vms2.macc.wisc.edu.

© 1995 by the Biophysical Society

0006-3495/95/06/2280/09 \$2.00

after double-affinity chromatography on oligo(dT) cellulose columns (Pharmacia, Piscataway, NJ) and used as a template for cDNA synthesis. After size selection for fragments greater than 500 bp, the cDNA was introduced into the Uni-ZAP vector (cDNA synthesis kit; Stratagene, La Jolla, CA), thereby generating a library of 9×10^6 independent clones after packaging. About 10^5 recombinant phages were plated and transferred onto nylon filters (GeneScreen Plus, DuPont NEN, Boston, MA) before screening with oligodeoxynucleotide probes derived from the sequence of internal fragments of purified helothermine (beginning at positions 126 or 11, respectively, Fig. 7 A). The sequences of the probes were: 5'-GGITGTGCIATIGCITA-(C/T)TGCCCGATCA(A/G)CCACITACAA (corresponding to amino acids 130–143); and 5'-AACCCGATCA(A/G)CA(A/G)ACIGA(A/G)ATACIGATAA(A/G)CACAAACA (corresponding to amino acids 13–26). Labeling was carried out using the polynucleotide kinase (Boehringer Mannheim, Indianapolis, IN) and [γ - ^{32}P]ATP (Amersham, Arlington Heights, IL). Hybridization and washing were conducted at 42°C in the buffers recommended by the manufacturer. A total of 33 clones giving positive signals after two rounds of screening were subjected to *in vivo* excision and checked for insert size. Ten candidate clones were sequenced, and the one bearing the longest helothermine cDNA insert was fully analyzed. The complete DNA sequence of both strands was determined by the dideoxy chain-termination method according to Sanger et al. (1977) using a Sequenase Version 2.0 kit (United States Biochemical, Cleveland, OH) and internal, helothermine cDNA-specific primers.

Sequence analysis of homologous proteins

Sequence analysis was performed using the University of Wisconsin GCG package according to Devereux et al. (1984). GenBank accession number of proteins found to be homologous to helothermine are shown in parenthesis; mouse CRISP-1/AEG-1 (LO5559) and CRISP-3/AEG-2 (LO5560) (Mizuki and Kasahara, 1992; Haendler et al., 1993); rat DE/AEG (PIR accession number A24609) (Brooks et al., 1986; Charest et al., 1988); human TPX1 (B33329) and mouse TPX-1 (A33329) (Kasahara et al., 1989; Mizuki et al., 1992); white-face hornet (*Dolichovespula maculata*) antigen 5/2 (PIR accession number A31085) (Fang et al., 1988); antigen 5 from paper wasp (*Polistes exclamans*; A37329) and eastern yellow jacket

(*Vespula maculifrons*; B37329) (Lu et al., 1993); red imported fire ant (*Solenopsis invicta*) venom allergen Sol i III (B37330) (Hoffman, 1993); tobacco PR-1a (PIR accession number S00513) (Cornelissen et al., 1987; Pfitzner et al., 1988); tomato PR P6 (S26239) (Van Kan et al., 1992); maize PR-like protein (S14969) (Casacuberta et al., 1991); barley PR-1 (S32002) (Muradov et al., 1993); mouse-ear cress (*Arabidopsis thaliana*) PR-1 (JQ1693) (Uknes et al., 1992); pSc7 (PIR accession number S27448) (Schuren et al., 1993).

Purification of SR

Skeletal heavy SR from rabbit leg and back muscle was prepared as described previously (Valdivia et al., 1992). Total cardiac microsomes were prepared from pig ventricular myocardium as described previously (Connelly and Coronado, 1994). [^3H]ryanodine binding was performed in duplicate samples (50 μg protein each) incubated for 120 min at 36°C in 0.1 ml of 7 nM [^3H]ryanodine, 0.2 M KCl, 20 mM Tris-HEPES, pH 7.2, 1 mM EGTA plus 1.25 mM CaCl_2 ($\approx 10 \mu\text{M}$ free Ca^{2+}). Specific [^3H]ryanodine binding under optimal conditions (1 M KCl, 100 μM Ca^{2+} , 5 mM ATP, 100 nM [^3H]ryanodine) was 15.5 ± 2.3 pmol/mg. [^3H]PN200–110 binding was performed in duplicate samples of rabbit skeletal muscle transverse tubules and cardiac microsomes incubated for 40 min at room temperature (22–24°C) in 0.4 nM [^3H]PN200–110, 50 mM Tris-Cl, pH 7.2, as described previously (Valdivia et al., 1990).

Planar bilayer recordings

Planar bilayer formation and recording was performed as described previously (Coronado et al., 1992). The *cis* (cytosolic) solution composed of 240 mM CsCH_3SO_3 , 10 mM CsCl, and 10 mM HEPES titrated with Tris to pH 7.2. The *trans* (luminal) solution was 40 mM CsCH_3SO_3 , 10 mM CsCl, and 10 mM HEPES titrated with Tris to pH 7.2. The contaminant-free Ca^{2+} of the *cis* solution was in the range of 1–3.6 μM and was measured by Ca^{2+} electrode.

Permeabilization of rat ventricular trabeculae and flash photolysis of nitr-5

Thin (150–180 μm in diameter), unbranched trabeculae were dissected from adult rat hearts and were placed for 30 min (22–24°C) in relaxing solution containing 50 $\mu\text{g}/\text{ml}$ saponin as described previously (Patel et al., 1994). Trabeculae were stretched to produce an initial resting tension of about 6–10% P_0 , i.e., the maximum active tension elicited in solution of pCa 4.5. The SR was loaded with Ca^{2+} , and the loaded Ca^{2+} was released subsequently by rapid photogeneration of trigger Ca^{2+} from nitr-5. This was done by sequentially bathing the trabeculae in: 1) Ca^{2+} -depleting solution containing 25 mM caffeine and 5 mM EGTA for 1 min; 2) Preactivating solution (PA1) for 1 min; 3) Preactivating solution (PA2) for 1 min. PA1 and PA2 reduced the Ca^{2+} -buffering capacity of the relaxing solution wetting the tissue; 4) Ca^{2+} -loading solution (L), containing 0.37 mM total Ca^{2+} buffered with 0.7 mM nitr-5, for 5 min. Trabeculae were then exposed to a flash of UV light (360 nm, 85–100 mJ) from a xenon flash lamp to generate trigger Ca^{2+} , which induced transient Ca^{2+} -induced Ca^{2+} release from the SR. Once the tension transient was completed, the residual Ca^{2+} content of the SR was assessed by placing the trabeculae in caffeine-activating solution containing 10 mM caffeine and 0.05 mM EGTA. Finally, the trabeculae were returned to relaxing solution for at least 2 min.

Relaxing, PA1, PA2, Ca^{2+} -depleting, and caffeine-activating solutions contained in mM: 100 BES, 25 creatine phosphate, 5.3 MgATP, 1 free Mg^{2+} , and 1 dithiothreitol. Ionic strength was 180 mM, and pH was 7.0 at 22°C. In addition, relaxing solution contained 5 mM EGTA and 2.6 mM potassium propionate; PA1 contained 0.1 mM EGTA and 16.8 mM potassium propionate; PA2 contained 0.01 mM EGTA and 17.1 mM potassium propionate; Ca^{2+} -depleting solution was relaxing solution plus 25 mM caffeine; caffeine-activating solution had 0.05 mM EGTA, 16.96 mM potassium propionate, and 10 mM caffeine. The Ca^{2+} -loading solution contained 100 mM

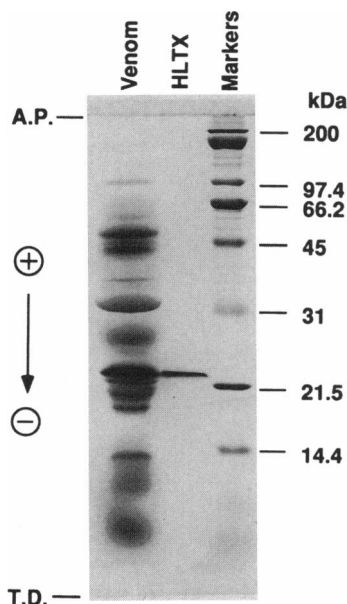


FIGURE 1 Electrophoretic analysis of purified helothermine. Coomassie Blue staining of SDS gel containing 12.5% polyacrylamide. (lane 1) 80 μg of soluble venom of *Heloderma horridum horridum*; (lane 2) 4 μg of purified helothermine (HLTX). (lane 3) Molecular weight markers. A.P. is the sample application point. T.D. marks the tracking dye.

BES, 14.5 mM creatine phosphate, 4 mM MgATP, 1 mM free Mg^{2+} , and 1 dithiothreitol plus 0.7 mM nitr-5 and 0.37 mM total Ca^{2+} and 56.9 mM potassium propionate. Assuming a K_d of 145 nM for nitr-5, the free Ca^{2+} in the loading solutions was calculated to be 160 nM.

Chemicals and abbreviations

[3H]ryanodine and [3H]PN200-110 (1 Ci/mmol) were from DuPont NEN. Nitr-5 and ryanodine were from Calbiochem (La Jolla, CA). Other reagents were from Sigma Chemical Co. (St. Louis, MO). BES (*N,N*-bis(2-hydroxyethyl)-2-aminoethanesulfonic acid; MES (2-[*N*-morpholino]ethane-sulfonic acid); PIPES (Piperazine-*N,N'*-bis-2-ethanesulfonic acid).

RESULTS AND DISCUSSION

Helothermine characterized in the present study was purified by gel exclusion and ion-exchange chromatography as a single polypeptide of molecular mass 25,500 Da (Fig. 1). After purification, the protein could be lyophilized without loss of toxic activity and was devoid of phospholipase A_2 activity, which is prominent in the crude venom (Sosa et al., 1986). Previous studies showed that the physiological effects observed in rodents injected with purified helothermine are lethargy, rear limb paralysis, hypothermia, and death (Mochca-Morales et al., 1990). The paralyzing effect suggested that one target of this toxin is excitation-contraction coupling. We investigated, therefore, whether helothermine was capable of interacting with receptors controlling this process. Dihydropyridine receptors in the plasma and transverse tubular membranes and ryanodine receptors in the junctional SR membrane are thought to be involved directly in excitation-contraction coupling of cardiac and skeletal muscle (McPherson and Campbell, 1993). Fig. 2 shows that

purified helothermine produced a strong inhibition of [3H]ryanodine binding to SR without affecting the binding of [3H]PN200-110 to skeletal or cardiac dihydropyridine receptors. Skeletal SR and transverse tubules (*circles*) and cardiac microsomes (*triangles*) were incubated with 7 nM [3H]ryanodine or 0.4 nM [3H]PN200-110 in the presence of the indicated concentrations of helothermine. The specific binding of [3H]ryanodine and [3H]PN200-110 in the absence of toxin was normalized to 100% in each case. Helothermine inhibited ~50% of the binding of [3H]ryanodine to skeletal SR at a concentration of 5 μg toxin/ml or ≈ 200 nM. The interaction of helothermine with the skeletal ryanodine receptor was complex because the dose-dependence curve (*filled circles*) consisted of at least two components. A high affinity component inhibited ~60% of [3H]ryanodine binding with an apparent toxin affinity of ≈ 20 nM. A component with a lower toxin affinity, inhibited [3H]ryanodine binding in the micromolar range. In cardiac SR, helothermine inhibited [3H]ryanodine binding in the micromolar range, and the dose-dependence curve was much steeper than in skeletal SR. The multiphasic toxin dose-dependence observed in skeletal SR and the highly steep dose-dependence observed in cardiac SR suggested that several interacting toxin binding sites are present in the ryanodine receptor.

We performed several receptor-binding and flux assays to determine whether helothermine selectively inhibited ryanodine receptors. As indicated above, [3H]PN200-110 binding to the cardiac or skeletal dihydropyridine receptor of the voltage-dependent Ca^{2+} channel was not affected by helothermine even at extremely high concentrations (Fig. 2). The lack of interaction of helothermine with the Ca^{2+} channel

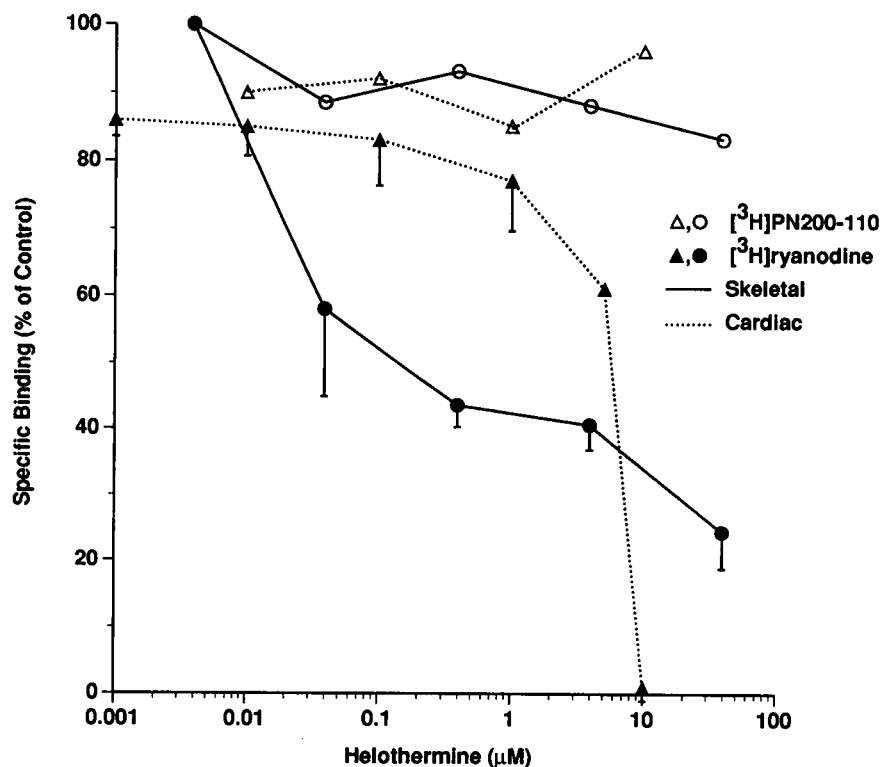


FIGURE 2 Displacement of [3H]ryanodine from skeletal and cardiac SR by helothermine. [3H]ryanodine binding in skeletal SR ($n = 4$) or cardiac SR ($n = 2$) and [3H]PN200-110 binding in skeletal transverse tubules ($n = 2$) or total cardiac microsomes ($n = 2$) was performed in the presence of the indicated helothermine concentrations.

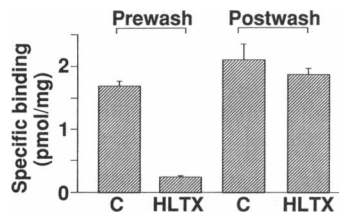


FIGURE 3 Reversible inhibition of [³H]ryanodine binding by helothermine. In prewash, skeletal SR was incubated for 15 min in binding buffer without (C) and with 10 μM helothermine (HLT) followed by incubation of both samples with 7 nM [³H]ryanodine. In postwash, skeletal SR was incubated during 15 min without (C) and with 10 μM helothermine (HLT) followed by pelleting and resuspension of both samples twice with binding buffer without toxin followed by incubation with 7 nM [³H]ryanodine.

dihydropyridine receptor was consistent with whole cell voltage-clamp studies, demonstrating that helothermine did not affect L-type Ca²⁺ currents in ventricular myocytes (Mochca-Morales et al., 1990). Other membrane currents of cardiac cells, such as the voltage-dependent Na⁺ current was not affected by helothermine as well (Mochca-Morales et al.,

1990). In addition, a concentration of 40 μM helothermine which, according to Fig. 2, inhibited 80% of [³H]ryanodine binding to skeletal receptors, did not affect the binding of 30 nM [³H]ouabain to the Na⁺/K⁺ pump of rabbit skeletal muscle transverse tubules (0.46 ± 0.05 pmol/mg in control and 0.51 ± 0.03 pmol/mg with toxin). ⁴⁵Ca²⁺ flux assays showed that 40 μM helothermine did not affect the rate of ATP-dependent Ca²⁺ uptake into rabbit skeletal muscle SR (1.2 ± 0.3 pmol/mg/min in control and 1.02 ± 0.25 pmol/mg/min with toxin). This result is consistent with experiments described below in which helothermine did not affect the rate of twitch relaxation after photolysis of caged Ca²⁺ in trabeculae of rat ventricle (Fig. 6). Taken together, these results suggested that helothermine interacted with ryanodine receptors in a rather selective manner because high concentrations of helothermine neither displaced drug binding from other muscle receptors nor affected the activity of the Ca²⁺ pump which, in skeletal muscle, is present at a much higher density than that of ryanodine receptors. As shown in Fig. 3, the inhibition of [³H]ryanodine binding was reversible as demonstrated by the fact that removal of helothermine by

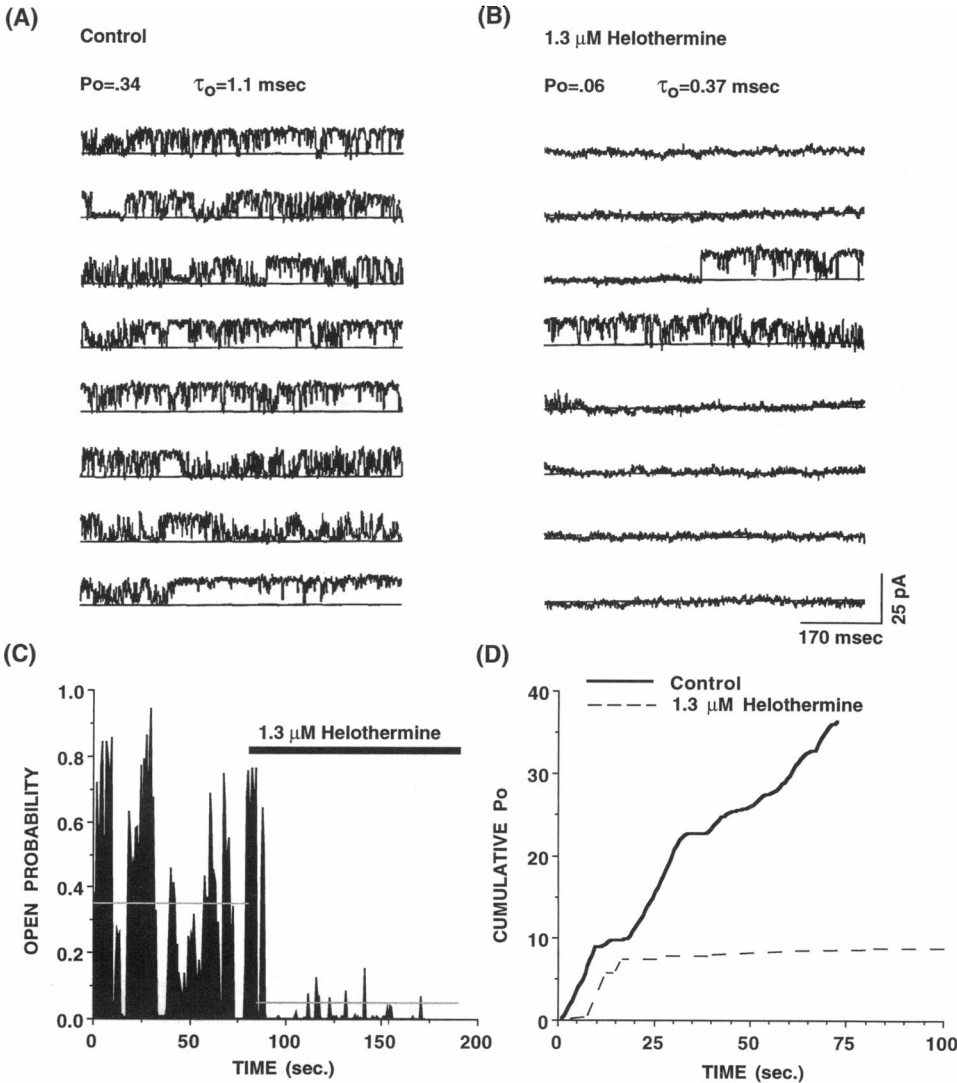


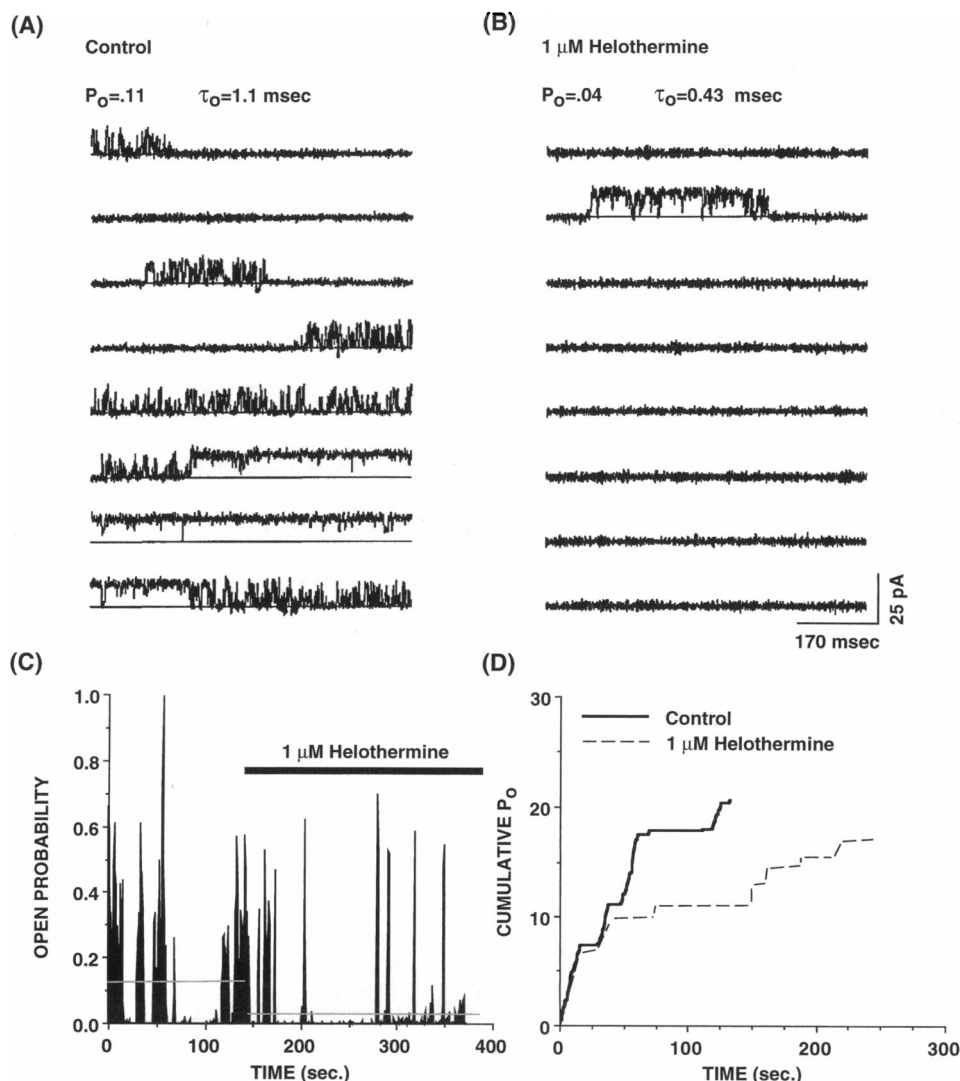
FIGURE 4 Block of skeletal ryanodine receptor by helothermine. Recordings from the same channel before (A) and after (B) *cis* addition of 1.3 μM helothermine at 0 mV. (C) A total of 160 s of continuous recordings before and after addition of helothermine were divided into 683 ms intervals. *P*_o in each interval is plotted as a bar of length 0 to 1. Average *P*_o during the control and test periods are indicated by the horizontal gray line. (D) A total of 80 s before and after addition of helothermine were divided into intervals of 683 ms. *P*_o in each interval was added to that of the previous one, and the cumulative sum was plotted as a function of recording time.

extensive wash of the SR sample before incubation with [^3H]ryanodine restored the binding activity to the control value.

The functional consequences of the interaction of helothermine with the ryanodine receptor were investigated in SR incorporated into planar bilayers. Fig. 4 shows the single-channel activity of a skeletal ryanodine receptor before and immediately after addition of toxin to the *cis* solution. Helothermine ($1.3\ \mu\text{M}$) produced a strong inhibition of activity manifested in a decrease in open probability and a decrease in mean open time. Open channel probability P_o was monitored during 80 s before and after toxin addition. Average P_o decreased approximately sixfold, from 0.34 during the control period to 0.06 during the test period. As shown in Fig. 4 *C* (bottom left), the most significant effect of helothermine was a decrease in the number of burst periods during which P_o remains at a relatively high level. The decrease in activity was quantified in Fig. 4 *D* (bottom right) as a graph of cumulative P_o as a function of recording time. In this plot, P_o was averaged during intervals of 683 ms for a total recording time of at least 75 s in each condition. The open probability

of each interval was added to that of the next interval, and the cumulative sum was plotted as a function of time. The slope of the plot is proportional to the number and duration of open events per unit time. From this plot, it is apparent that helothermine produced a constant inhibition that was not relieved with time of exposure. The inhibition by helothermine resulted in a decrease in the mean open channel duration from 1.1 to 0.37 ms and a significant increase in the mean closed channel duration (not shown). The same protocol was used in Fig. 5 to demonstrate block of a cardiac ryanodine receptor from porcine SR. At approximately the same concentration of toxin used for skeletal channels ($1\ \mu\text{M}$), helothermine produced a twofold decrease in the P_o of the cardiac channel during the same monitoring period. Thus, the inhibition of the cardiac ryanodine receptor by helothermine was much weaker than that of the skeletal channel. In addition, a comparison of Figs. 4 *D* and 5 *D* indicated that the inhibition of the cardiac channel had a longer lag period than that of the skeletal channel. The much stronger blockade of skeletal ryanodine receptors by micromolar helothermine was consistent with the dose-response curves of [^3H]ryano-

FIGURE 5 Block of cardiac ryanodine receptor by helothermine. Recordings from the same channel before (A) and after (B) *cis* addition of $1\ \mu\text{M}$ helothermine at 0 mV. (C) A total of 400 s of continuous recordings before and after addition of helothermine were divided into 683-ms intervals. P_o in each interval is plotted as a bar of length 0 to 1. Average P_o during control and test periods are indicated by the horizontal gray line. (D) A total of 150 s before, and 250 s after, addition of helothermine were divided into intervals of 683 ms. P_o in each interval was added to that of the previous one, and the cumulative sum was plotted as a function of recording time.



dine binding (Fig. 2), which indicated that $1 \mu\text{M}$ helothermine inhibited a much larger percent of alkaloid binding to the skeletal than to the cardiac receptor. The underlying mechanism of channel inhibition by helothermine appeared to be similar in cardiac and skeletal receptors because, in both cases, there was a decreased mean open duration and the appearance of long quiescent periods. The fact that open times were strongly affected by helothermine tended to rule out a mechanism of inhibition based on an occlusion on the open channel, as described for K^+ channel toxins (Valdivia et al., 1988). However, it is possible that helothermine lowers the Ca^{2+} sensitivity of the channel because this mechanism will also inhibit the binding of $[^3\text{H}]$ ryanodine to the receptor.

To determine whether helothermine was capable of blocking ryanodine receptors in situ, we investigated the effect of the toxin on the release of Ca^{2+} from the SR of saponin-permeabilized ventricular trabeculae of rat myocardium. SR Ca^{2+} release was assessed by measurements of isometric tension and was induced by a trigger Ca^{2+} generated as a result of flash photolysis of nitr-5 (Patel et al., 1995). Fig. 6A shows photolysis-induced tension transients recorded in the absence and presence of $1 \mu\text{M}$ helothermine. In the presence of helothermine, there was a 50% reduction in the amplitude of the tension transient elicited by flash photolysis. In control experiments, the amplitude of the tonic tension generated by pCa 4.5 as well as the caffeine-elicited tension transient, remained unaffected by helothermine (data not shown). This indicated that the decrease in the amplitude of the tension transient produced by helothermine was due neither to a decrease in the Ca^{2+} sensitivity of the myofilament nor to a decrease in the amount of Ca^{2+} available for release. Furthermore, Fig. 6B indicated that the kinetics of the tension transient after flash photolysis of nitr-5 were not affected by helothermine. Because the rate of rise and fall of tension reflects the rate of rise and fall of the Ca^{2+} transient (Endoh and Blinks, 1988), this result would indicate that helothermine selectively decreased the number of release sites affecting neither the kinetics of activation of the Ca^{2+} release channel nor the kinetics of Ca^{2+} re-uptake by the Ca^{2+} pump.

The complete amino acid sequence of helothermine as deduced after the cloning of the corresponding cDNA is shown in Fig. 7A. Five stretches of this sequence (represented in **bold**) were originally obtained by amino acid determination of fragments generated by chemical cleavage or tryptic digestion. Oligodeoxynucleotide probes were synthesized according to the peptidic sequence and were used to screen a cDNA library, constructed from salivary gland mRNA of *Heloderma horridum horridum*. This allowed us to isolate a full length helothermine cDNA clone. DNA sequencing revealed the presence of a 1104-nucleotide-long insert (not shown; GenBank accession number U13619) containing an open reading frame coding for a 242-amino-acid protein, which included all of the stretches previously determined by peptide cleavage. A hydrophobic signal peptide of 19 amino acids was present in the precursor as deduced from the N-terminal sequence of the mature protein. No potential N-glycosylation site was found. A salient feature of

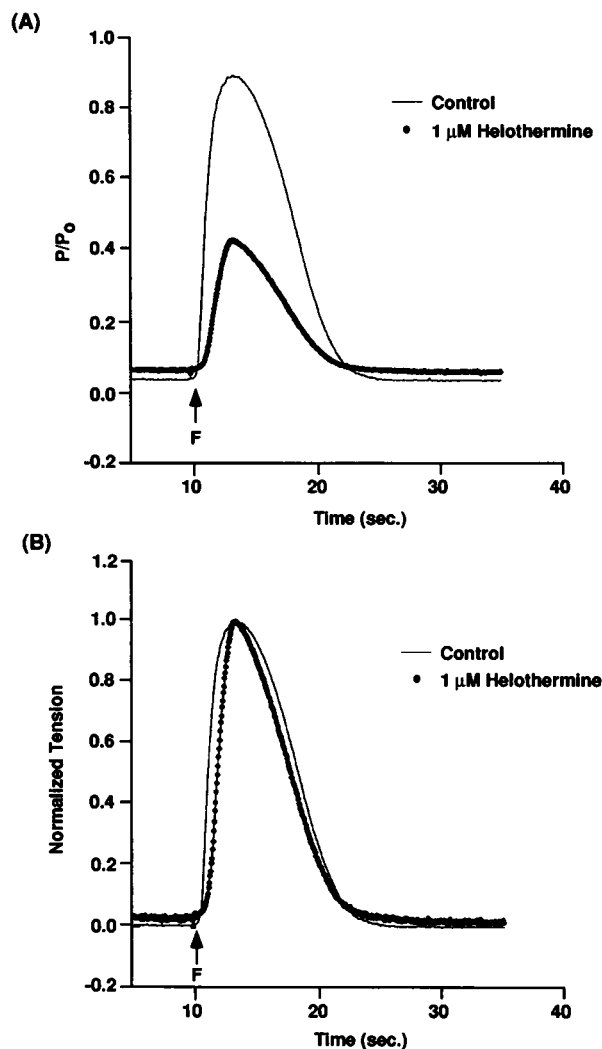


FIGURE 6 Inhibition by helothermine of SR Ca^{2+} release initiated by flash photolysis of nitr-5 in saponin-permeabilized ventricular trabeculae. Trabeculae were incubated for 5 min in loading solution ($375 \mu\text{M}$ Ca^{2+} , $700 \mu\text{M}$ nitr-5) with and without $1 \mu\text{M}$ helothermine. The time before the flash (F) corresponds to the last 10 s of the loading period. (A) Tension is relative to the maximum tension generated by the trabeculae at pCa 4.5. (B) Tension is relative to the peak tension after photolysis.

the protein is its unusual richness in cysteine residues (a total of 16 for the mature protein), with 10 of them clustered in the C-terminal 54 residues.

None of the known Na^+ , K^+ , or Ca^{2+} channel-specific toxins recently cataloged (Adams and Swanson, 1994) were found to share structural similarities with helothermine. However, a number of proteins not known to affect channels exhibited significant homology with helothermine (Fig. 7B). The highest identities were found with a family of cysteine-rich secretory proteins (CRISP) described in human and mouse testis (TPX1 and Tpx-1; 49.6 and 46.7%), mouse salivary gland (CRISP-3, alternative name AEG-2; 41.5%), and mouse and rat epididymis (CRISP-1/AEG-1 and DE/AEG; 45.5% and 46.3%) (Brooks et al., 1986; Charest et al., 1988; Kasahara et al., 1989; Mizuki and Kasahara, 1992; Mizuki et al., 1992; Haendler et al., 1993). Helothermine and CRISP

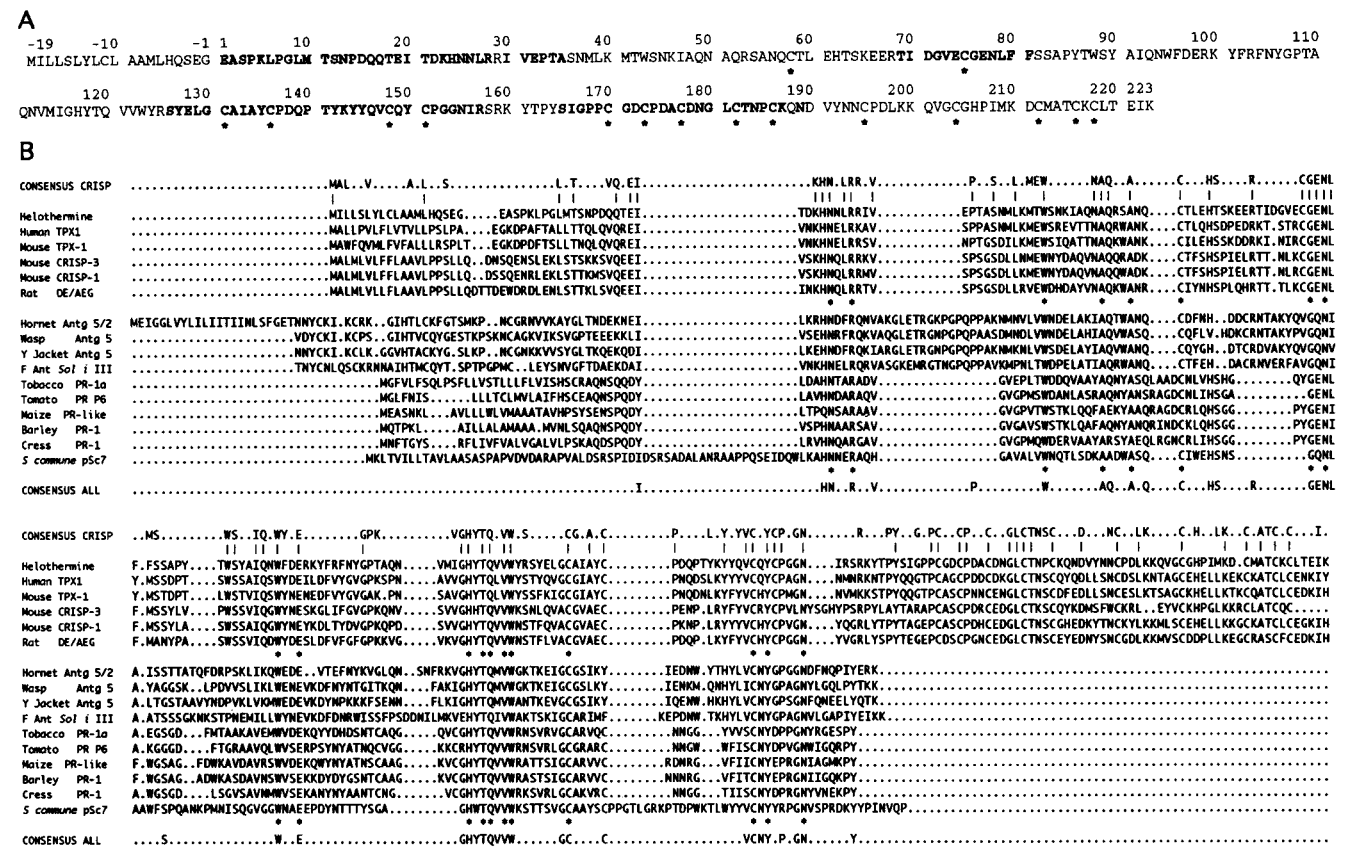


FIGURE 7 Amino acid sequence of helothermine deduced from the cDNA nucleotide sequence (GenBank accession number U13619). (A) Boldface letters indicate amino acid residues determined by Edman degradation of the purified protein (residues 1–20) and of isolated peptide fragments obtained after tryptic digestion (69–81, 126–143, 144–157, and 165–189) or cyanogen bromide cleavage (11–35). The 16 cysteine residues of the mature protein are highlighted by asterisks. (B) Amino acid sequence alignment of helothermine with the other known members of the CRISP family and with the more distantly related proteins of the antigen 5/Sol i III, pathogenesis-related protein 1, and pSc7 from basidiomycete fungus *Schizophyllum commune*. The upper consensus line shows residues conserved in at least five of the six CRISPs, and vertical bars indicate residues invariant within the CRISP family. Entries in the lower consensus line indicate positions with agreement in at least 10 of the 16 protein sequences, whereas asterisks mark the 19 invariant residues of the superfamily.

proteins share 16 invariant cysteine residues that are suggestive of a common pattern of disulfide bridges. A weaker, but still significant, similarity exists with insect venom sac proteins of the antigen 5/Sol i III family (Fang et al., 1988; Lu et al., 1993; Hoffmann et al., 1993a, b), with pathogenesis-related proteins from various plants (Cornelissen et al., 1987; Pfizner et al., 1988; Casacuberta et al., 1991; Van Kan et al., 1992; Uknes et al., 1992; Muradov et al., 1993), and with the fruit body-specific proteins from the basidiomycete fungus *Schizophyllum commune* (Schuren et al., 1993). These insect, plant, and fungus proteins lack the cysteine-rich C-terminal moiety characteristic of the CRISP family. In addition, only three out of the six cysteine residues of the N-terminal moiety of helothermine and CRISP proteins were invariant in the antigen 5, PR, and pSc proteins. On the other hand, all of the proteins shared a common core stretch (GHYTVQVW) corresponding to residues 116–123 of helothermine.

Although proteins related to helothermine appear to be present in basidiomycete fungus, plants, insects, and mammals, their function(s) is virtually unknown. In mammals, the epididymal glycoprotein CRISP-1 (DE/AEG) appears to be involved in sperm maturation (Brooks et al., 1986; Charest

et al., 1988; Kasahara et al., 1989; Mizuki et al., 1992; Mizuki and Kasahara, 1992; Haendler et al., 1993). In plants, a partial resistance against pathogenic comycete fungi has been observed for transgenic tobacco constitutively expressing pathogenesis-related protein PR-1a (Alexander et al., 1993). Here we identified helothermine as a new member of the CRISP family of proteins and suggested that the ryanodine receptor is a target of this protein in striated muscle. Because CRISP proteins are present in mammalian tissues, the possibility that CRISP-like proteins endogenously regulate ryanodine receptors must also be considered.

With regard to the toxic action of helothermine in rodents, it is unlikely that exogenous helothermine reaches ryanodine receptors in muscle unless it is assisted by other components of *Heloderma* venom, such as phospholipase A₂ (Sosa et al., 1986), to facilitate diffusion of helothermine across the surface membrane. Also, it should be excluded that a membrane-permeable fragment of helothermine produced by cleavage of the whole protein penetrates muscle cells to produce a direct block of the ryanodine receptor. In cell membrane-free preparations such as skinned muscle cells used here, helothermine should become a powerful probe of

ryanodine receptor structure and function because helothermine was capable of overriding Ca^{2+} -dependent activation of SR Ca^{2+} release.

This work was supported by National Institutes of Health grant GM 36852 and HL25861, Schering AG, Howard Hughes Medical Institute Award 75191-52704, American Heart Association, and Muscular Dystrophy Association of America.

REFERENCES

- Adams, M. E., and G. Swanson. 1994. Neurotoxins. *Trends Neurosci.* 17: 1s-28s.
- Alexander, D., R. M. Goodman, M. Gut-Rella, C. Glascock, K. Weymann, L. Friedrich, D. Maddox, P. Ahl-Goy, T. Lintz, E. Ward, and J. Ryals. 1993. Increased tolerance to two mycete pathogens in transgenic tobacco expressing pathogenesis-related protein 1a. *Proc. Natl. Acad. Sci. USA.* 90:7327-7331.
- Brooks, D. E., A. R. Means, E. J. Wright, S. P. Singh, and K. K. Tiver. 1986. Molecular cloning of the cDNA for androgen-dependent sperm coating glycoproteins secreted by the rat epididymis. *Eur. J. Biochem.* 161:13-18.
- Callaway, C., A. Seryshev, J.-P. Wang, K. J. Slavik, D. J. Needleman, C. Cantu, Y. Wu, T. Jayaraman, A. R. Marks, and S. L. Hamilton. 1994. Localization of the high and low affinity [^3H]ryanodine binding sites on the skeletal muscle Ca^{2+} release channel. *J. Biol. Chem.* 269:15876-15884.
- Casacuberta, J. M., P. Puigdomenech, and B. San Segundo. 1991. A gene coding for a basic pathogenesis-related (PR-like) protein from Zea mays. Molecular cloning and induction by a fungus (*Fusarium moniliforme*) in germinating maize seeds. *Plant Mol. Biol.* 16:527-536.
- Charest, N. J., D. R. Joseph, E. M. Wilson, and F. S. French. 1988. Molecular cloning of complementary deoxyribonucleic acid for an androgen-regulated epididymal protein: sequence homology with metalloproteins. *Mol. Endocrinol.* 2:999-1004.
- Chen, S. R. W., L. Zhang, and D. H. MacLennan. 1992. Characterization of a Ca^{2+} binding and regulatory site in the Ca^{2+} release channel (ryanodine receptor) of rabbit skeletal muscle sarcoplasmic reticulum. *J. Biol. Chem.* 267:23318-23326.
- Connelly, T. J., and R. Coronado. 1994. Activation of the Ca^{2+} release channel of cardiac sarcoplasmic reticulum by volatile anesthetics. *Anesthesiology.* 81:459-469.
- Cornelissen, B. J. C., J. Horowitz, J. A. L. van Kan, R. B. Goldberg, and J. F. Bol. 1987. Structure of tobacco genes encoding pathogenesis-related proteins from the PR-1 group. *Nucleic Acids Res.* 15:6799-6811.
- Coronado, R., S. Kawano, J. C. Lee, C. Valdivia, and H. H. Valdivia. 1992. Planar bilayer recording of ryanodine receptors of sarcoplasmic reticulum. *Methods Enzymol.* 207:699-707.
- Coronado, R., J. Morrisette, M. Sukhareva, and D. M. Vaughan. 1994. Invited review: structure and function of ryanodine receptors. *Am. J. Physiol.* 35:C1485-C1504.
- Devereux, J., P. Haerberli, and O. Smithies. 1984. A comprehensive set of sequence analysis programs for the VAX. *Nucleic Acids Res.* 12:387-395.
- Endoh, M., and J. R. Blinks. 1988. Actions of sympathomimetic amines on the Ca^{2+} transients and contractions of rabbit myocardium: reciprocal changes in myofibrillar responsiveness to Ca^{2+} mediated through α - and β -adrenoreceptors. *Circ. Res.* 62:247-265.
- Fang, K. S. Y., M. Vitale, P. Fehlner, and T. P. King. 1988. cDNA cloning and primary structure of a white-face hornet venom allergen, antigen 5. *Proc. Natl. Acad. Sci. USA.* 85:895-899.
- Giangiaco, K. M., E. E. Sugg, M. Garcia-Calvo, R. J. Leonard, O. B. McManus, G. J. Kaczorowski, and M. L. Garcia. 1993. Synthetic charybdotoxin-I berotoxin chimeric peptides define toxin binding site on calcium-activated and voltage-dependent potassium channels. *Biochemistry.* 32:2363-2370.
- Haendler, B., J. Krättschmar, F. Theuring, and W.-D. Schleuning. 1993. Transcripts for cysteine-rich secretory protein-I (CRISP-I; DE/AEG) and the novel related CRISP-3 are expressed under androgen control in the mouse salivary gland. *Endocrinology.* 133:192-198.
- Hoffman, D. R. 1993a. Allergens in Hymenoptera venom XXIV: the amino acid sequences of imported fire ant venom allergens Sol i II, Sol i III, and Sol i IV. *J. Allergy Clin. Immunol.* 91:71-78.
- Hoffman, D. R. 1993b. Allergens in Hymenoptera venom XXV: the amino acid sequences of antigen 5 molecules and the structural basis of antigenic cross-reactivity. *J. Allergy Clin. Immunol.* 91:707-716.
- Kasahara, M., J. Gutknecht, K. Brew, N. Spurr, and P. N. Goodfellow. 1989. Cloning and mapping of a testis-specific gene with sequence similarity to a sperm-coating glycoprotein gene. *Genomics.* 5:527-534.
- Lu, G., M. Villalba, M. R. Coscia, D. R. Hoffman, and T. P. King. 1993. Sequence analysis and antigenic cross-reactivity of a venom allergen, antigen 5, from hornets, wasps, and yellow jackets. *J. Immunol.* 150: 2823-2830.
- MacKinnon, R., and C. Miller. 1989. Mutant potassium channels with altered binding of charybdotoxin, a pore-blocking peptide inhibitor. *Science.* 245:1382-1385.
- Martin, B. M., E. Carbone, A. Yatani, A. M. Brown, A. N. Ramirez, G. B. Gurrola, and L. D. Possani. 1988. Amino acid sequence and physiological characterization of toxins from the venom of the scorpion *Centruroides limpidus tecomanus* Hoffmann. *Toxicon.* 26:785-794.
- McPherson, P. S., and K. P. Campbell. 1993. The ryanodine receptor/ Ca^{2+} release channel. *J. Biol. Chem.* 268:13765-13768.
- Mizuki, N., and M. Kasahara. Mouse submandibular glands express an androgen-regulated transcript encoding an acidic epididymal glycoprotein-like molecule. 1992. *Mol. Cell. Endocrinol.* 89:25-32.
- Mizuki, N., D. E. Sarapata, J. A. Garcia-Sanz, and M. Kasahara. 1992. The mouse male germ cell-specific gene Tpx-1: molecular structure, mode of expression in spermatogenesis, and sequence similarity to two non-mammalian genes. *Mamm. Genome.* 3:274-280.
- Mochca-Morales, J., B. M. Martin, and L. D. Possani. 1990. Isolation and characterization of helothermine, a novel toxin from *Heloderma horridum* (Mexican beaded lizard) venom. *Toxicon.* 28:299-309.
- Muradov, A., L. Petrasovits, A. Davidson, and K. J. Scott. 1993. A cDNA clone for a pathogenesis-related protein 1 from barley. *Plant Mol. Biol.* 23:439-442.
- Otsu, K., H. F. Willard, V. K. Khanna, F. Zorzato, N. M. Green, and D. H. MacLennan. 1992. Molecular cloning of cDNA encoding the Ca^{2+} release channel (ryanodine receptor) of rabbit cardiac muscle sarcoplasmic reticulum. *J. Biol. Chem.* 265:13472-13483.
- Patel, J. R., R. Coronado, and R. L. Moss. 1995. Cardiac sarcoplasmic reticular phosphorylation increases calcium release by flash photolysis of nitr-5. *Circ. Res.* In press.
- Pfützner, U. M., A. J. P. Pfützner, and H. M. Goodman. 1988. DNA sequence analysis of a PR-1a gene from tobacco: molecular relationship of heat shock and pathogen responses in plants. *Mol. Gen. Genet.* 211:290-295.
- Possani, L. D., B. M. Martin, I. Svendsen, G. S. Rode, and B. W. Erickson. 1985. Scorpion toxins from *Centruroides noxius* and *Tityus serrulatus*. *Biochem. J.* 229:739-750.
- Possani, L. D., B. M. Martin, A. Yatani, J. Mochca-Morales, F. Z. Zamudio, G. B. Gurrola, and A. M. Brown. 1992. Isolation and physiological characterization of taicatoxin, a complex toxin with specific effects on calcium channels. *Toxicon.* 30:1343-1364.
- Sambrook, J., E. F. Fritsch, and T. Maniatis. 1989. Molecular Cloning: A Laboratory Manual, 2nd ed. Cold Spring Harbor Laboratory Press, Cold Spring Harbor, NY. 18-22.
- Sanger, F., S. Nicklen, and A. R. Coulson. DNA sequencing with chain-terminating inhibitors. 1977. *Proc. Natl. Acad. Sci. USA.* 74:5463-5467.
- Schuren, F. H. J., S. A. Asgeirsdottir, E. M. Kothe, J. M. J. Scheer, and J. G. H. Wessels. 1993. The Sc7/Sc14 gene family of Schizophyllum commune codes for extracellular proteins specifically expressed during fruit-body formation. *J. Gen. Microbiol.* 139:2083-2090.
- Sosa, B. P., A. C. Alagon, B. M. Martin, and L. D. Possani. 1986. Biochemical characterization of the phospholipase A_2 from the venom of the Mexican beaded lizard (*Heloderma horridum horridum* Wiegmann). *Biochemistry.* 25:2927-2933.
- Sorrentino, V., and P. Volpe. 1993. Ryanodine receptors: how many, where, and why. *Trends Pharmacol. Sci.* 14:98-103.
- Uknes, S., B. Mauch-Mani, M. Moyer, S. Potter, S. Williams, S. Dincher, D. Chandler, A. Slusarenko, E. Ward, and J. Ryals. 1992. Acquired resistance in Arabidopsis. *Plant Cell.* 4:645-656.

- Valdivia, H. H., and R. Coronado. 1990. Internal and external effects of dihydropyridines in the calcium channel of skeletal muscle. *J. Gen. Physiol.* 95:1–27.
- Valdivia, H. H., O. Fuentes, J. Morrisette, and R. Coronado. 1991. Activation of sarcoplasmic reticulum Ca^{2+} release channels by a novel scorpion venom peptide. *J. Biol. Chem.* 266:19135–19138.
- Valdivia, H., M. Kirby, J. Lederer, and R. Coronado. 1992. Scorpion toxins specifically targeted against the intracellular Ca^{2+} release channel of skeletal and cardiac muscle. *Proc. Natl. Acad. Sci. USA.* 89:12185–12189.
- Valdivia, H. H., J. S. Smith, B. M. Martin, R. Coronado, and L. D. Possani. 1988. Charybdotoxin, and Noxiustoxin, two homologous peptide blockers of the K(Ca) channel. *FEBS Lett.* 226:280–284.
- Valdivia, C., D. M. Vaughan, B. V. L. Potter, and R. Coronado. 1992. Fast release of Ca^{2+} by inositol 1,4,5-trisphosphate and Ca^{2+} in the sarcoplasmic reticulum of skeletal muscle. *Biophys. J.* 61:1184–1193.
- Van Kan, J. A. L., M. H. A. J. Joosten, C. A. M. Wagemakers, G. C. M. van den Berg-Velthuis, and P. J. G. M. de Wit. 1992. Differential accumulation of mRNAs encoding extracellular and intracellular PR proteins in tomato induced by virulent and avirulent races of *Cladosporium fulvum*. *Plant Mol. Biol.* 20:513–527.
- Wagenknecht, T., R. Grassucci, J. Frank, A. Saito, M. Inui, and S. Fleischer. 1989. Three dimensional architecture of the calcium channel/foot structure of sarcoplasmic reticulum. *Nature.* 338:167–170.
- Wang, J. P., D. H. Needleman, and S. H. Hamilton. 1993. Relationship of low affinity [^3H]ryanodine binding sites to high affinity sites on the skeletal muscle Ca^{2+} release channel. *J. Biol. Chem.* 268:20974–20982.